


MiR-887-3p Negatively Regulates STARD13 and Promotes Pancreatic Cancer Progression

This article was published in the following Dove Press journal:
Cancer Management and Research

Xiaobo Xu
Shusen Zheng 

Division of Hepatobiliary and Pancreatic Surgery, Department of Surgery, First Affiliated Hospital, School of Medicine, Zhejiang University, Hangzhou, Zhejiang, People's Republic of China

Purpose: STARD13 is regulated by various miRNAs. However, there are relatively few reports describing the relationship between miRNAs and STARD13 in pancreatic cancer. Therefore, the aim of this study was to explore the relationship between miRNA and STARD13 in pancreatic cancer.

Patients and Methods: By analyzing the data from Gene Expression Omnibus (GEO) database, the relationship between STARD13 expression and pancreatic cancer was explored. Then, through sequence alignment, the sequence complementary to miR-887-3p in the 3'UTR of STARD13 mRNA was found, mutated and cloned. Dual-luciferase reporter assay was used to test the relationship between STARD13 and miR-887-3p. Pancreatic cancer tumor tissue and its adjacent tissues collected, and the expression of STARD13 and miR-887-3p in pancreatic cancer tissues was analyzed by RT-qPCR. After, miR-887-3p and its inhibitor were transfected into PANC-1 cells to further confirm the regulatory relationship between miR-887-3p and STARD13 by RT-qPCR, and CCK-8, colony formation assays, cell cycle analysis, apoptosis detection and transwell analysis were used to detect changes of proliferation, apoptosis, migration and invasion in PANC-1 cells. Finally, through in vivo experiments, the effect of miR-887-3p on tumor growth was researched.

Results: We found that STARD13 expression is lower in pancreatic cancer tissues, with the level of miR-887-3p being higher in these tissues. Pancreatic cancer patients with particularly low levels of STARD13 presented with a poor prognosis. MiR-887-3p negatively regulates the expression of STARD13. Increasing levels of miR-887-3p decreased the expression of STARD13, which promoted the proliferation, cell cycle process, cell migration and invasion, and inhibited the apoptosis of pancreatic cancer cells. Inhibition of miR-887-3p in SCID mice could inhibit tumor growth and promote tumor cell apoptosis.

Conclusion: In conclusion, STARD13 is negatively regulated by miR-887-3p in pancreatic cancer. MiR-887-3p may act to promote cancer progression, and as such, it is a viable target for intervention and diagnostic development.

Keywords: microRNAs, StAR-related lipid transfer protein 13, pancreatic cancer, miR-887-3p, poor prognosis

Introduction

With its ever-increasing incidence in China, pancreatic cancer is now one of the top 10 tumors associated with cancer-related deaths across the globe.¹ In the United States, it is predicted that pancreatic cancer will surpass breast cancer as the second deadliest tumor by 2030.² According to the 2009 Shanghai Epidemiological Research Statistics report, the incidence of pancreatic cancer in men and women in Shanghai is 17.28/100,000 and 14.04/100,000, respectively.³ According to recent statistics from the National Cancer Center, the incidence of pancreatic cancer in

Correspondence: Shusen Zheng
Division of Hepatobiliary and Pancreatic Surgery, Department of Surgery First Affiliated Hospital, School of Medicine, Zhejiang University, No. 79 Qingchun Road, Hangzhou, Zhejiang 310003, People's Republic of China
Tel + 86 571 87236466
Email shusenzheng@zju.edu.cn

China rose to ninth place in 2015, and the mortality rate places it in sixth place in terms of deaths.² The annual changes in morbidity and mortality rates are 1.3 and 1.2, respectively, and the overall morbidity and mortality continue to increase every year.¹ Pancreatic cancer is currently the most malignant solid tumor with its 5-year survival rate at only about 6%.^{4,5} Thus, there is a critical need for the identification of novel targets to assist in the development of new surveillance and intervention strategies worldwide. This global interest means that there is a significant amount of novel research being conducted on pancreatic cancer throughout the world.

MicroRNAs (miRNAs) are endogenous non-coding RNA transcripts encoded by various genes, consisting of relatively stable 22 to 23 nucleotides, identified in most peripheral blood and bodily fluids.^{6–8} They regulate gene expression by binding to their target mRNA within the 3'-untranslated region (UTR), and are key regulators in a number of cellular functions including cell proliferation, differentiation, metastasis, and apoptosis.^{6,7,9} Many studies have shown that the expression of some miRNAs is related to the occurrence, development and prognosis of various different types of tumors.^{7,10} Studies have shown that the combination of miR-887 and miR-3619 can abolish more than 90% of phospholipase D (PLD) enzyme activity, thereby reducing the invasion ability of breast cancer cells.¹¹ Several other studies have shown that miRNA can be used as a biomarker for tumor diagnosis and prognosis.^{6,12–15} In addition, Yan Jiang found a significant increase in the level of miR-887-5p in the serum of patients with endometrial cancer, and believed that miR-887-5p in serum may be a potential biomarker for the diagnosis and prognosis of endometrial cancer.⁷

StAR-related lipid transfer protein 13 (STARD13), also known as deleted in liver cancer 2 (DLC2) and located on chromosome 13q12.3, is the GTPase-activating protein for Rho and has been shown to act as a tumor suppressor.^{6,16–18} It is expressed at low levels in various tumors including lung cancer, kidney cancer, breast cancer and colon tumors.^{6,19–21} The ceRNA network moieties associated with STARD13 have been shown to inhibit migration, invasion, and epithelial mesenchymal transformation (EMT) of breast cancer.^{6,22} STARD13 is targeted by several miRNAs which play key roles in regulating tumor progression.⁶ MiRNA-125b targets STARD13 and NEU1 to improve the invasion and metastasis of gastric cancer cells,^{6,23} while in triple-negative breast cancer, miR-9 directly targets STARD13.^{6,24} Thus, we wanted to evaluate

the potential roles of miR-887 and STARD13 in the progression of pancreatic cancers and establish the regulatory relationship between them.

In this study, we investigated the roles of miR-887-3p and STARD13 in the development of pancreatic cancer and studied the regulatory relationship between them.

Patients and Methods

Bioinformatics Analysis

Genome-wide expression profiling of 118 pancreatic ductal adenocarcinoma (PDAC) samples and 13 control samples, and mRNA expression profiling of 7 pairs of matched pancreatic cancer patient samples were downloaded from the Gene Expression Omnibus (GEO) database (<https://www.ncbi.nlm.nih.gov/geo/>). GraphPad Prism 8.2.1 was used to analyze the differences in STARD13 expression in normal and pancreatic cancer tissues. Pancreatic cancer patients were divided into two groups based on their expression of STARD13, low STARD13 and high STARD13. Kaplan-Meier (KM) curve analysis was then used to compare the survival rates of these two groups.

Patients and Tissue Samples

Pancreatic cancer tissues (n = 5) and their adjacent non-tumorous tissues (n = 5) were obtained from the First Affiliated Hospital of College of Medicine, Zhejiang University. After removed from the human body, these tissues were immediately frozen in liquid nitrogen and then stored at –80°C until RNA extraction. Ethical approval for this study was obtained from the Independent Ethics Committee of the First Affiliated Hospital of College of Medicine, Zhejiang University. Informed and written consent was obtained from all patients or their appointed representative in accordance with the ethics committee guidelines.

Cell Lines

PANC-1 (catalog number: CRL-1469) and HEK293 (catalog number: CRL-1573) were purchased from the American Type Culture Collection (ATCC) (Washington, DC, United States) and cultured in DMEM (GIBCO, catalog number: 11965–092, Shanghai, China) containing 10% fetal bovine serum (FBS) (GIBCO, catalog number: 10091–148, Shanghai, China) and 1% penicillin-streptomycin solution (GIBCO, catalog number: 15070–063, Shanghai, China).

Real-Time Quantitative PCR (RT-qPCR)

RNA was extracted from tissue homogenates or cells using Trizol (Ambion, catalog number: 15596-026, Shanghai, China) and reverse transcribed to cDNA using Hiscript Reverse Transcriptase (VAZYME, catalog number: R101-01/02, Nanjing, Jiangsu, China). Reverse transcription of the target miRNA was completed using an hsa-miR-887-3p specific primer and a loop primer (Table 1). This cDNA was then used for RT-qPCR using an SYBR Green Master Mix (VAZYME, catalog number: Q111-02, Nanjing, Jiangsu, China) to determine relative RNA expression. The primers used in this RT-qPCR analysis are shown in Table 1.

Dual-Luciferase Reporter Assays

Wild type or mutant copies of the hSTARD13 3'UTR were cloned into a pYr-MirTarget vector (Hunan Changsha Yingrun Biotechnology Co., Ltd., Changsha, Hunan, China), and named STARD13 3'UTR-WT and STARD13 3'UTR-MUT, respectively. The mutation in the STARD13 3'UTR-MUT sequence is shown in red letters in Figure 1D. HEK293 cells were incubated overnight in 24-well plates at a density of 5×10^4 cells per well. STARD13 3'UTR-WT or STARD13 3'UTR-MUT were co-transfected into the HEK293 cells with the negative control of miR-887-3p mimic (mimic NC) or miR-887-3p mimic using Lipofectamine 2000 (Invitrogen, catalog number: 11668-019, Shanghai, China) according to the manufacturer's instructions. Dual-luciferase reporter assays (Promega, catalog number: E1910, Beijing, China) were performed 48 h after transfection using the manufacturer's instructions. Differences in transfection efficiency

were normalized by dividing the firefly luciferase activity by the values for the Renilla luciferase.

Cellular Proliferation Assays

PANC-1 cells were cultured overnight in 96-well plates at a density of 5×10^3 cells per well. MiR-887-3p mimic and inhibitor, and their corresponding negative control was transfected into PANC-1 cells using Lipofectamine 2000. After 48 h, 10 μ L of CCK-8 (BIOSHARP, catalog number: BS350B, Beijing, China) was added to each well and the plates were cultured for a further 4 h. The results of this assay were collected by measuring absorbance at OD450 on a microplate reader.

Colony Formation Assays

PANC-1 cells treated with miR-887-3p mimic or miR-887-3p inhibitor were evenly spread across the 6-well plates, reaching a density of 500 cells per well. After 3 weeks, the culture medium was discarded, and the cells were fixed in 4% formaldehyde. The fixed cells were then stained with Giemsa for 30 min, and photographed using a light microscope and counted.

Cell Cycle Assays

PANC-1 cells were evenly plated and incubated in 6-well plates overnight. After treated with miR-887-3p mimic or miR-887-3p inhibitor for 48 h, the cells were collected and fixed in 70% ethanol at 4°C overnight. After two washes with PBS, the fixed cells were incubated in PBS supplemented with 0.2% Triton X-100 and 10 μ g/mL RNase at 37°C for 30 mins. Then, these cells were stained with propidium iodide (PI, 50 μ g/mL) (Nanjing kaiji biotechnology development co. LTD, catalog number: KGA512,

Table 1 Details of the RT-qPCR and Loop Primers

Name of Primers	Sequence (5'-3')	Gene ID
U6-F U6-R	CGCTTCGGCAGCACATATAC AAATATGGAACGCTTCACGA	26827
hsa-miR-887-3p-Loop hsa-miR-887-3p-F hsa-miR-887-3p-R	GTCGTATCCAGTGCAGGGTCCGAGGTATTCGCACTGGATACGACCCTCGGGA TGCGCGTGAACGGGCGCCATCC CCAGTGCAGGGTCCGAGGTATT	100126347
GAPDH-F GAPDH-R	TCAAGAAGGTGGTGAAGCAGG TCAAAGGTGGAGGAGTGGGT	2597
STARD13-F STARD13-R	ACTGTCTGTGGTGGGAAACA TGAGGCACACTTGTTCACG	90627

Nanjing, Jiangsu, China) at 4°C for 30 mins in the dark and analyzed using a flow cytometer.

Apoptosis Assays

PANC-1 cells were cultured overnight in 6-well plates at a density of 5×10^5 cells per well. After treated with miR-887-3p mimic or miR-887-3p inhibitor for 48 h, both adherent and floating cells were collected and washed with PBS. These cells were then stained using Annexin V-FITC and PI (Nanjing kaiji biotechnology development co. LTD, catalog number: KGA108, Nanjing, Jiangsu, China) in the dark for 10 min at room temperature. Subsequent analysis was performed on a flow cytometer. The results are presented as the percentage of apoptotic cells relative to the total number of cells in this analysis.

Transwell Assays

After PANC-1 cells were cultured overnight, miR-887-3p mimic and inhibitor, or their corresponding negative control was transfected into PANC-1 cells using Lipofectamine 2000. After 48 h, the cells were used for Transwell analysis. Migration was measured using Matrigel-free transwell plates with an 8 μ m porous membrane and invasion was measured using transwell plates with Matrigel. Cells were inoculated into the upper chamber of transwell plates at a density of 4×10^3 cells per well; 200 μ L of serum-free medium was added to the upper chamber and 500 μ L of medium supplemented with 10% FBS was added to the lower chamber. After 24 hrs of incubation, cellular migrating or invasion was evaluated using 0.5% crystal violet staining. Images were captured using a light microscope and invasive/motile cells were counted.

Adenovirus Preparation

The miR-887-3p inhibitor was cloned into an adenovirus shuttle vector and co-transfected with the auxiliary packaging plasmid pBHG lox Δ E1,3 Cre (Microbix, Shanghai, China) into HEK293 cells using SunBio Trans-EZ (Shanghai shengbo biomedical technology co., LTD, catalog number: STP07009, Shanghai, China). These cells were used to propagate and prepare adenovirus expressing an inhibitor of miR-887-3p (AV-miR-887-3p inhibitor). At the same time, an empty adenovirus shuttle vector was transfected into HEK293 cells with pBHG lox Δ E1 and 3 Cre, preparing adenovirus expressing the negative control of miR-887-3p inhibitor (AV-Vector). When most of the cells showed typical pathological changes, and 50% of the

cells were desiccated, the cells were collected, frozen and thawed three times at -70°C and 37°C and the supernatant was collected as raw viral extract. After virus purification,²⁵ the titer of virus was determined,²⁶ and the virus stored at -70°C .

Animal Experiments

Animal studies were performed at the Zhejiang University's animal center. Laboratory animals were used in accordance with the Principles of Laboratory Animal Care (NIH no. 85-23, 1985 version). All experiments using animals were performed in accordance with a protocol approved by the Ethical Committee on Animal Experiments from the Animal Care and Use Committee at Zhejiang University.

Six male SCID mice aged 6–8 weeks were purchased from Beijing Huafukang Biotechnology Co., Ltd., and were housed in pathogen-free transparent plastic cages under a constant 12 hrs light-dark cycle with free access to water and chow. All mice were acclimatized for 1 week prior to the start of the experiment and the mice were euthanized when their single tumor volume reached 1500 mm³ and/or they became moribund (weight loss of >15% of their initial weight, a lack of grooming, cachexia). At the end of the study, all male SCID mice used in this research were placed in the euthanasia chamber, and 100% CO₂ gas was introduced at a flow rate of 30–70% of the chamber volume per minute. When no corneal reflex, detectable breathing, or heartbeat was observed for more than 5 mins, the animals were confirmed dead. All efforts were made to minimize animal suffering.

To produce the tumor model, 5×10^7 PANC-1 cells were inoculated subcutaneously into the left chest of each male SCID mouse. Tumor volume was measured every 3 to 4 days after the first week, and six male SCID mice were randomly divided into the AV-Vector group where 1×10^9 PFU AV-Vector was injected into the tail vein twice a week, and the AV-miR-887-3p inhibitor group where 1×10^9 PFU AV-miR-887-3p inhibitor was injected into the tail vein twice a week. After 3 weeks, the mice were euthanized, and the tumor was removed.

Hematoxylin-Eosin (HE) Staining Analysis

Murine tumors were made into paraffin sections.²⁷ After dewaxing the sections were sequentially stained with Mayer's hematoxylin (Sigma, catalog number: H9627, Shanghai, China) and a 1% water-soluble eosin stain

(Sinopharm Group, catalog number: 71,014,544, Shanghai, China), magnified under the microscope and then photographed 200 times.

TUNEL Detection Assays

The tumors were placed in paraffin and sectioned as described above. After dewaxing, the sections were sequentially stained using an apoptosis detection kit (Shanghai Yisheng Biotechnology Co., Ltd., catalog number: 40308ES20, Shanghai, China) and DAPI (Beyotime, catalog number: C1002, Shanghai, China), and then photographed as described above.

Statistical Analysis

SPSS 22.0 (IBM SPSS, Armonk, NY, USA) was used for all statistical analyses. Comparisons between two groups were performed using a student's *t* test (unpaired). Comparisons between multiple groups were performed using analysis of variance (ANOVA). $P < 0.05$ indicates a statistically significant difference, and graphs were drawn using GraphPad Prism 8.2.1 (GraphPad Software, Inc., La Jolla, California, United States). Data is representative of at least 3 independent experiments and shown as mean \pm standard deviation (SD).

Results

STARD13 Transcription Is Reduced in Pancreatic Cancer Tissues

Analysis of the GEO data revealed that STARD13 transcription in pancreatic cancer tissues was lower than that of normal tissues (Figure 1A and B), and the survival rates of pancreatic cancer patients with low STARD13 transcription levels were lower than those with higher STARD13 levels (Figure 1C). These observations were confirmed by similarly decreased STARD13 transcription in the pancreatic cancer tissue samples collected during this study (Figure 1D). These results show that STARD13 mRNA levels decreased in pancreatic cancer tissues, and patients with low levels of STARD13 mRNA had poor prognosis.

MiR-887-3p Regulates the Level of STARD13 mRNA

The tissue samples we collected were analyzed by RT-qPCR and we found that miR-887-3p expression was higher in pancreatic cancer tissues than in normal tissues (Figure 1D). Sequence alignment revealed that

there is a miR-887-3p recognition sequence in the 3'UTR of STARD13 (Figure 1E). To determine if this is an active regulatory sequence, STARD13 3'UTR-WT or STARD13 3'UTR-MUT was then co-transfected with miR-887-3p into PANC-1 cells. The dual-luciferase reporter assays revealed that miR-887-3p reduced the expression of STARD13 wild type without affecting the expression of the STARD13 mutant (Figure 1F), which confirms that miR-887-3p can regulate the expression of STARD13, and revealed the binding site of this regulation. MiR-887-3p mimic and miR-887-3p inhibitor was separately transfected into PANC-1 cells, and STARD13 expression was evaluated using RT-qPCR. This analysis demonstrated that increasing miR-887-3p expression was linked to decreasing STARD13 expression (Figure 1G and H). These results indicate that miR-887-3p acts as a negative regulator of STARD13 expression in pancreatic cancer.

MiR-887-3p Promotes the Proliferation and Cell Cycle Process of PANC-1 Cells

MiR-887-3p mimic and miR-887-3p inhibitor and their corresponding controls were transfected into PANC-1 cells. CCK-8, colony formation and cell cycle analyses revealed that the overexpression of miR-887-3p promotes cellular proliferation (Figure 2A), increases colony formation (Figure 2B and 2C), and promotes cell cycle process (Figure 2D and E). These data suggest that increasing miR-887-3p expression improves the overall proliferation capacity and cell cycle process of pancreatic cancer cells.

MiR-887-3 Inhibits Apoptosis, and Promotes Cell Migration and Invasion in PANC-1 Cells

PANC-1 cells transfected with miR-887-3p mimic and inhibitor and their relevant controls were subjected to apoptosis and transwell analysis which revealed that the inhibition of miR-887-3p expression improved cellular apoptosis (Figure 3A and B) and suppressed cellular migration and invasion (Figure 3C-F). Overexpression of miR-887-3p resulted in the opposite effect. These data indicate that increased expression of miR-887-3p may inhibit apoptosis and promote cellular migration and invasion in pancreatic cancer.

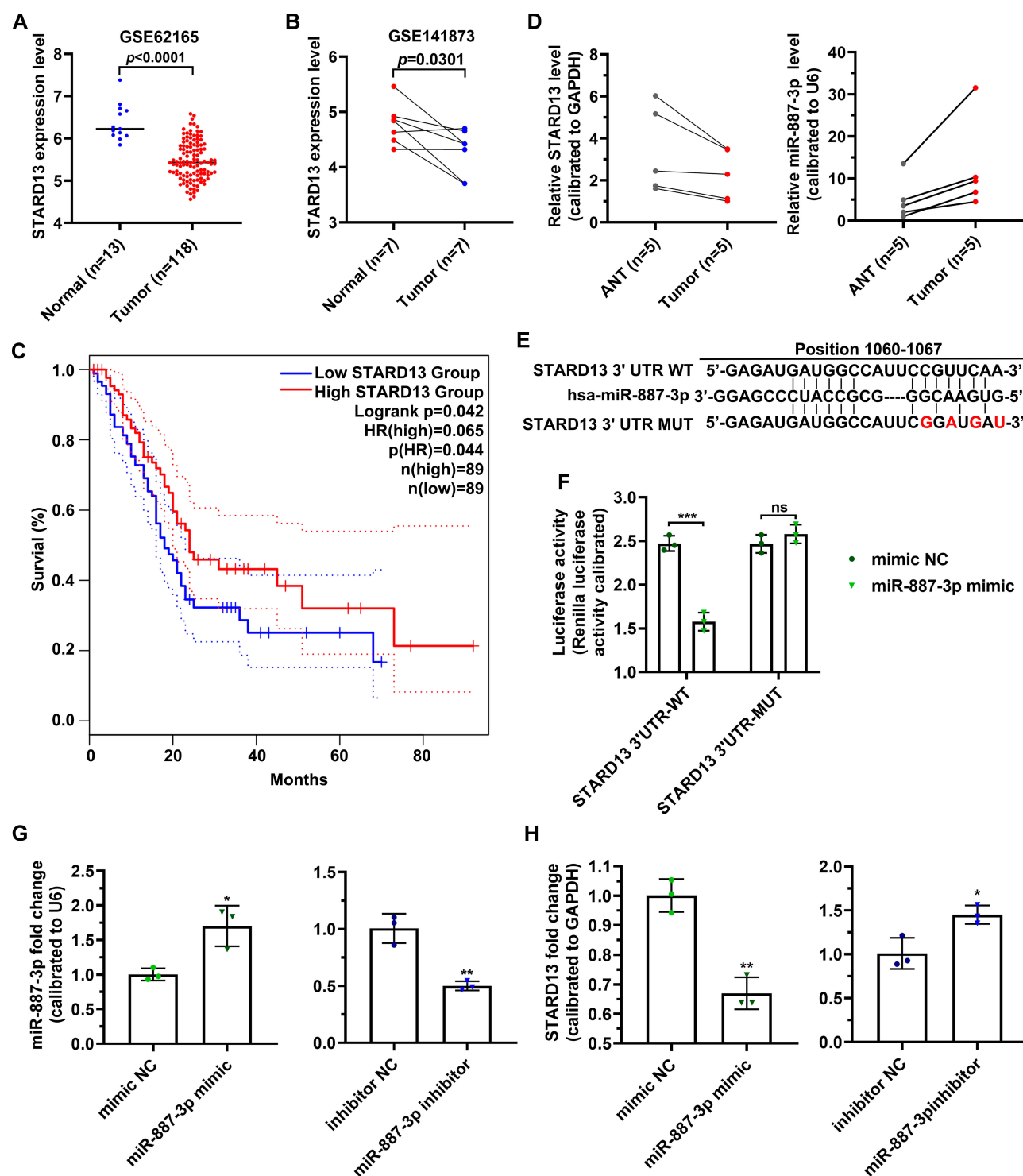


Figure 1 STARD13 expression is reduced in pancreatic cancer tissues and miR-887-3p regulates STARD13 mRNA. (A) GEO data (GEO accession: GSE62165) was used to analyze the expression of STARD13 in normal and PDAC tissues. (B) Transcription data from GEO (GEO accession: GSE141873) was used to compare the level of STARD13 in pancreatic cancer and adjacent normal tissues. (C) The correlation analysis between STARD13 expression level in patients with pancreatic cancer and overall survival rates was done using KM curves analysis. (D) The levels of STARD13 and miR-887-3p in pancreatic cancer tissues and corresponding adjacent normal tissues was evaluated by RT-qPCR. (E) Schematic diagram of the STARD13 3'UTR point mutation created in this study. (F) STARD13 3'UTR-WT or STARD13 3'UTR-MUT were co-transfected into HEK293 cells with mimic NC or miR-887-3p mimic. The regulatory relationship between miR-887-3p and STARD13 was analyzed using a Dual-luciferase reporter assay system. (G-H) Mimic NC, miR-887-3p mimic, the negative control of miR-887-3p inhibitor (inhibitor NC), and miR-887-3p inhibitor were serially transfected into PANC-1 cells. STARD13 (G) and miR-887-3p (H) expression in these cells was evaluated by RT-qPCR. ANT: adjacent normal tissues; mimic NC: the negative control of miR-887-3p mimic; inhibitor NC: the negative control of miR-887-3p inhibitor; STARD13 3'UTR WT: the wild type of STARD13 3'-untranslated region; STARD13 3'UTR MUT: the mutant of STARD13 3'-untranslated region; STARD13 3'UTR-WT: plasmid expressing the wild type of STARD13 3'-untranslated region was transfected into cells; STARD13 3'UTR-MUT: plasmid expressing the mutant of STARD13 3'-untranslated region was transfected into cells; ns, not significant; *: $p < 0.05$; **: $p < 0.01$; ***: $p < 0.001$.

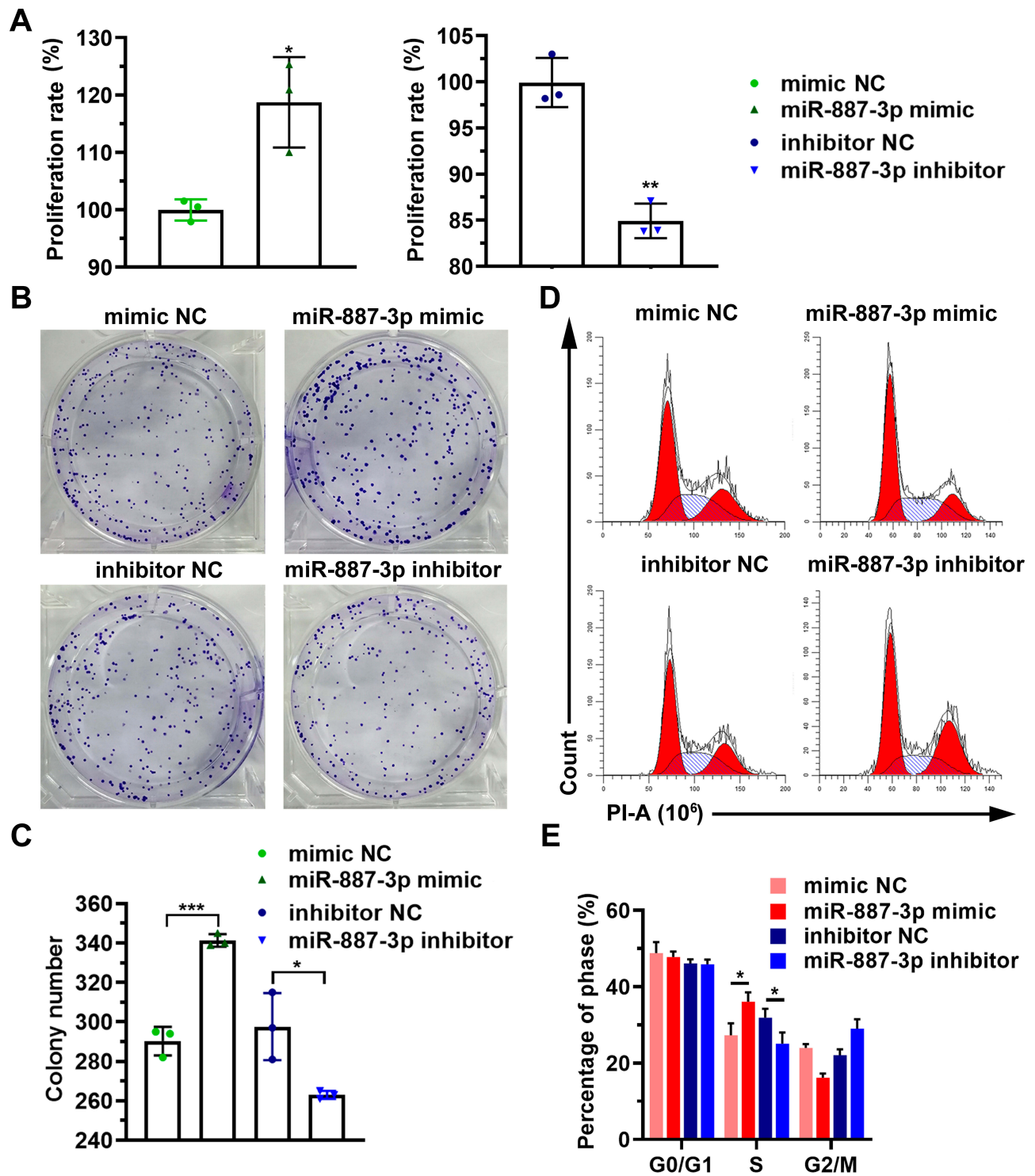


Figure 2 MiR-887-3p promotes the proliferation and cell cycle process of PANC-1 cells. Mimic NC, miR-887-3p mimic, inhibitor NC, and miR-887-3p inhibitor were serially transfected into PANC-1 cells. **(A)** The proliferation of the cells was analyzed using a CCK-8 assay. **(B)** The effect of miR-887-3p on colony formation was examined using a colony formation assay. **(C)** Histogram describing the number of colonies formed under each condition. **(D)** Cell cycle analysis following miR-887-3p treatment in PANC-1 cells. **(E)** Histogram describing the proportion of cells in different stages of the cell cycle under different treatments. Mimic NC: the negative control of miR-887-3p mimic; inhibitor NC: the negative control of miR-887-3p inhibitor; *: $p < 0.05$; **: $p < 0.01$; ***: $p < 0.001$.

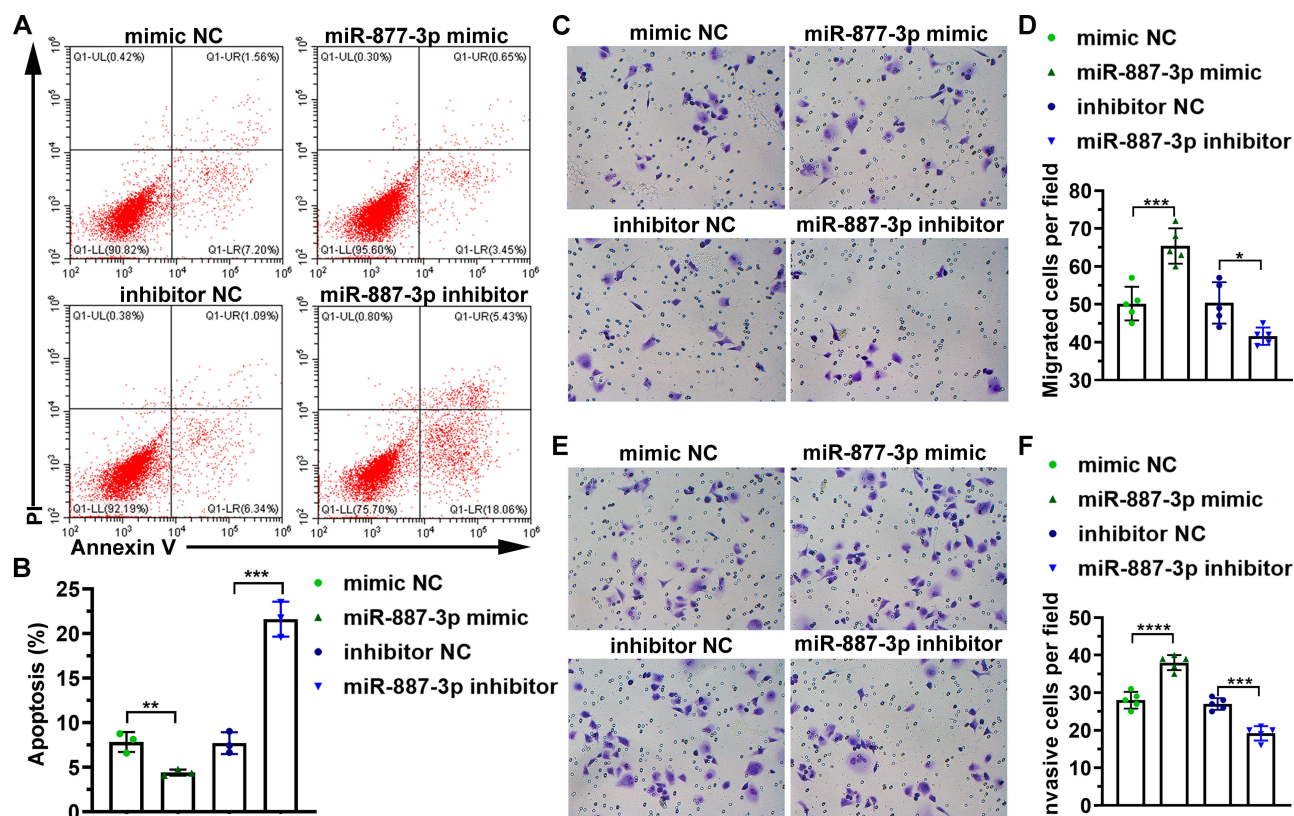


Figure 3 MiR-887-3 inhibits apoptosis, and promotes cellular migration and invasion in PANC-1 cells. Mimic NC, miR-887-3p mimic, inhibitor NC, and miR-887-3p inhibitor were serially transfected into PANC-1 cells. (A) Annexin V-FITC and PI staining was used to detect the effect of miR-887-3p on apoptosis. (B) Histogram describing the percentage of apoptosis under various treatment conditions. (C–F) Transwell analysis was used to examine the effect of miR-887-3p on cellular migration (C and D) and invasion (E and F). Mimic NC: the negative control of miR-887-3p mimic; inhibitor NC: the negative control of miR-887-3p inhibitor; *: $p < 0.05$; **: $p < 0.01$; ***: $p < 0.001$; ****: $p < 0.0001$.

Inhibiting MiR-887-3p Expression Suppresses Tumor Growth and Promotes Apoptosis in vivo

We found that miR-887-3p targets STARD13 mRNA and inhibits its expression, thereby promoting the growth, migration, and invasion of pancreatic cancer cells in vitro. We then confirmed these findings in vivo. SCID mice were inoculated with PANC-1 cells and given AV-miR-887-3p inhibitor after tumor formation. We found that treatment with AV-miR-887-3p inhibitor increased the transcription of STARD13 in SCID mice (Figure 4A) and inhibited tumor growth (Figure 4B and C). After tumor removal, HE staining and TUNEL assay revealed that treatment with AV-miR-887-3p inhibitor promoted apoptosis of cells inside the tumor (Figure 4D–F). These findings suggest that inhibiting the expression of miR-887-3p increased the expression of STARD13, thereby inhibiting tumor growth and promoting cell apoptosis in pancreatic cancer samples. This suggests that miR-887-3p is a potential target for the treatment of pancreatic cancer.

Discussion

Pancreatic cancer is known as the “king of cancer” and is the most malignant gastrointestinal tumor.^{28–30} After diagnosis, the 5-year survival rate of patients is less than 8%.³¹ Therefore, it is necessary to develop a better understanding of the regulation of pancreatic cancer progression in order to provide novel targets for the diagnosis and treatment of these malignancies. In the current study, we found that in pancreatic cancer, STARD13 is low in expression indicating a poor prognosis, miR-887-3p is highly expressed, and miR-887-3p negatively regulates STARD13. These findings provide direction and basis for further research on miR-887-3p as a target for pancreatic cancer.

MiRNA plays a crucial role in the development and progression of tumors via various complex mechanisms.^{32,33} Studies have shown that miRNA expression can be used to distinguish normal and cancerous tissues and some specific miRNAs have been found to be closely related to the diagnosis and prognosis of specific cancers.^{33,34} This means that

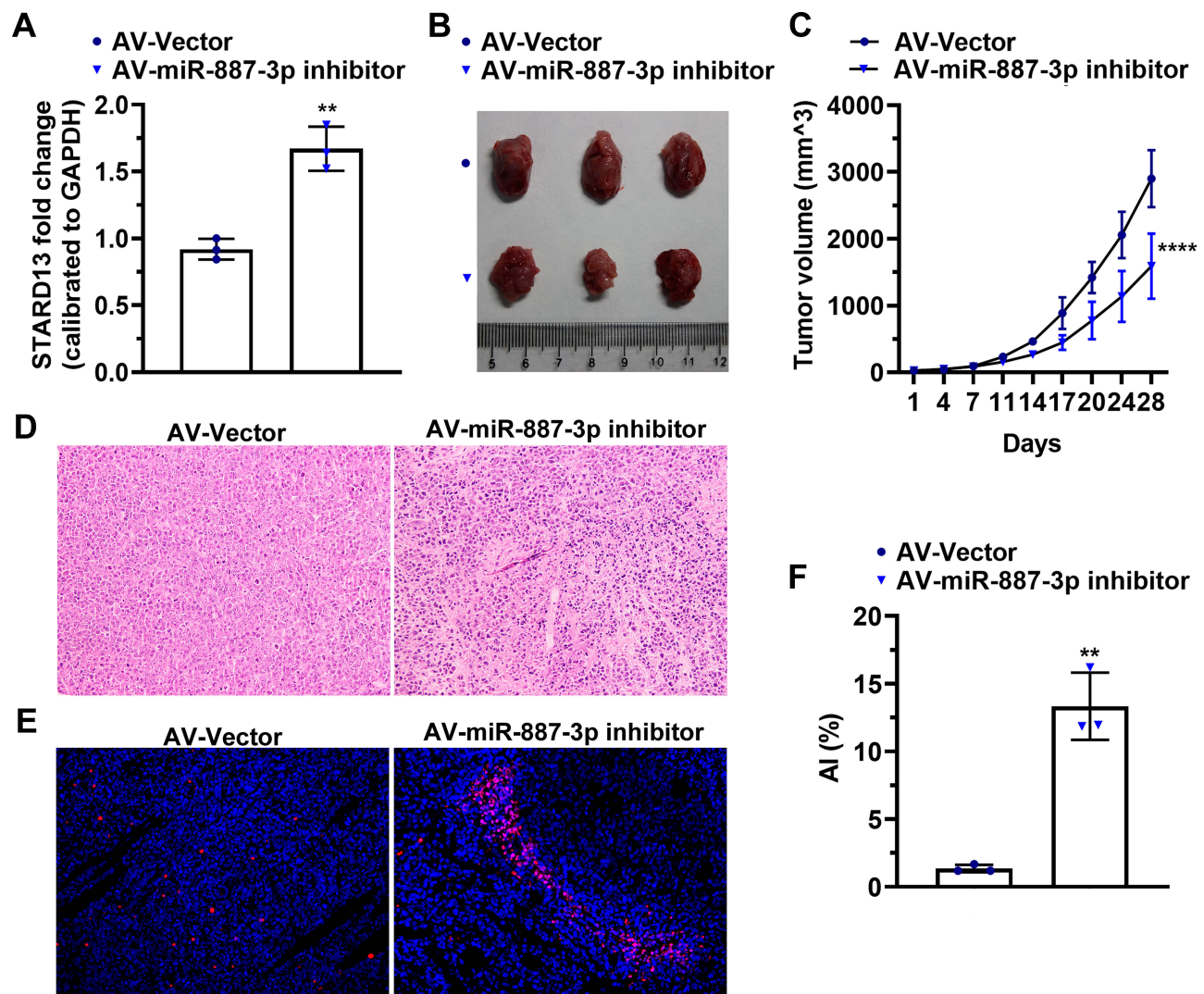


Figure 4 In vivo inhibition of miR-887-3p suppresses tumor growth and promotes apoptosis. PANC-1 cells were inoculated subcutaneously into SCID mice. After 1 week, six male SCID mice were randomly divided into two treatment groups AV-Vector Group which was treated with 1×10^9 PFU AV-Vector, and AV-miR-887-3p inhibitor Group which was treated with 1×10^9 PFU AV-miR-887-3p inhibitor. (A) After tumor excision, STARD13 transcription was evaluated by RT-qPCR. (B) After the tumor was removed, the size of the tumors was measured. (C) Statistical curve for tumor volume at different times. (D) Images of the tumor tissues after HE staining. (E) Images of the tumor tissues after TUNEL staining. (F) Histogram of apoptosis rates in the tumor tissues following treatment. AV-Vector: adenovirus expressing the negative control of miR-887-3p inhibitor; AV-miR-887-3p inhibitor: adenovirus expressing an inhibitor of miR-887-3p; **: $p < 0.01$; ****: $p < 0.0001$.

miRNAs have great potential for application in the diagnosis, prognosis and treatment of various tumors. In our study, we found that miR-887-3p is highly expressed in pancreatic cancer tissues, promoting proliferation, migration, and invasiveness of PANC-1 cells, and tumor growth. Likewise, some researchers have found that the level of miR-887-5p in the serum of patients with endometrial cancer is significantly increased suggesting that serum miR-887-5p levels could be used as a potential biomarker for endometrial cancer.⁷ In addition, studies have shown that miR-887-3p targets the MDM4 3'-UTR, resulting in reduced expression of MDM4 increasing the risk of small cell lung cancer.³⁵ Whereas, we testified that miR-887-3p targets the STARD13 3'-UTR,

leading to decreased STARD13 expression and promoting pancreatic cancer progression. Moreover, STARD13 has been proven to exert inhibitory effects on liver, prostate, lung, breast, kidney, and colon cancers,^{6,19-21} which is consistent with those of previous studies.

In breast cancer cells, overexpression of miR-887 can inhibit PLD expression and enzyme activity, thereby reducing the aggressiveness of breast cancer cells.¹¹ Nevertheless, in pancreatic cancer cells, overexpression of miR-887-3p improved cell invasiveness. Furthermore, studies have shown that miR-191-5p and miR-887-3p can only inhibit the expression of MDM4 in small cell lung cancer cells with the C allele rather than A allele.³⁵ These

data demonstrate the complexity of the roles of miRNA in cancer and cellular homeostasis. These findings also indicate that miR-887 may play different roles when cooperating with different molecules in different tumor tissues. These also suggest that the details of miR-887-3p's negative regulation of STARD13 to promote pancreatic cancer progression need to be further studied.

In addition, there are some limitations to the study. Only one cell line was used and the expression patterns of miR-887-3p and STARD13 in different pancreatic cell lines were not investigated. Our study is lack of rescue experiments to directly prove the key role of STARD13 in the promotive effects of miR-887-3p on pancreatic cancer cells.

Conclusion

In conclusion, this study found that miR-887-3p promotes pancreatic cancer progression and negatively regulates STARD13. Moreover, STARD13 has been shown to function as a tumor suppressor suggesting that miR-887-3p may promote tumor progression by negatively regulating STARD13 in pancreatic cancer. This finding provides a direction and basis for more extensive analysis of this dynamic and the potential application of miR-887-3p as a diagnostic, prognostic, or therapeutic target in the future.

Data Sharing Statement

All relevant data and materials are presented in the manuscript. For more information, please contact the corresponding author.

Ethics Approval and Informed Consent

Ethical approval for this study was obtained from the Independent Ethics Committee of the First Affiliated Hospital of College of Medicine, Zhejiang University. Informed and written consent was obtained from all patients or their appointed representative in accordance with the ethics committee guidelines.

All experiments using animals were performed in accordance with a protocol approved by the Ethical Committee on Animal Experiments from the Animal Care and Use Committee at Zhejiang University.

Acknowledgments

Thanks to Research on Application of Public Welfare Technology in Zhejiang Province (Experimental Animals) for funding (2017C37102). We are very grateful to patients who agreed to provide tumor tissue.

Author Contributions

SZ designed the study, collected the patients' tissues, analyzed the data from GEO. XX is responsible for related cell experiments and animal experiments. All authors contributed to data analysis, drafting or revising the article, gave final approval of the version to be published, and agree to be accountable for all aspects of the work.

Funding

This work was supported by Research on Application of Public Welfare Technology in Zhejiang Province (Experimental Animals) (2017C37102).

Disclosure

The authors report no conflicts of interest in this work.

References

- Chen W, Zheng R, Baade PD, et al. Cancer statistics in China, 2015. *CA Cancer J Clin.* 2016;66(2):115–132. doi:10.3322/caac.21338
- Rahib L, Smith BD, Aizenberg R, Rosenzweig AB, Fleshman JM, Matrisian LM. Projecting cancer incidence and deaths to 2030: the unexpected burden of thyroid, liver, and pancreas cancers in the United States. *Cancer Res.* 2014;74(11):2913–2921. doi:10.1158/0008-5472.CAN-14-0155
- Long J, Luo GP, Xiao ZW, et al. Cancer statistics: current diagnosis and treatment of pancreatic cancer in Shanghai, China. *Cancer Lett.* 2014;346(2):273–277. doi:10.1016/j.canlet.2014.01.004
- Siegel RL, Miller KD, Jemal A. Cancer statistics, 2015. *CA Cancer J Clin.* 2015;65(1):5–29. doi:10.3322/caac.21254
- Neumann CCM, von Horschelmann E, Reutzel-Selke A, et al. Tumor-stromal cross-talk modulating the therapeutic response in pancreatic cancer. *Hepatobil Pancreatic Dis Int.* 2018;17(5):461–472. doi:10.1016/j.hbpd.2018.09.004
- Chen L, Hu W, Li G, Guo Y, Wan Z, Yu J. Inhibition of miR-9-5p suppresses prostate cancer progress by targeting StarD13. *Cell Mol Biol Lett.* 2019;24:20. doi:10.1186/s11658-019-0145-1
- Jiang Y, Wang N, Yin D, et al. Changes in the expression of serum MiR-887-5p in patients with endometrial cancer. *Int J Gynecol Cancer.* 2016;26(6):1143–1147. doi:10.1097/IGC.00000000000000730
- Bogen KT. Efficient tumorigenesis by mutation-induced failure to terminate microRNA-mediated adaptive hyperplasia. *Med Hypotheses.* 2013;80(1):83–93. doi:10.1016/j.mehy.2012.10.017
- Zhi F, Wang S, Wang R, Xia X, Yang Y. From small to big: microRNAs as new players in medulloblastomas. *Tumour Biol.* 2013;34(1):9–15. doi:10.1007/s13277-012-0579-9
- Bueno MJ, Pérez de Castro I, Malumbres M. Control of cell proliferation pathways by microRNAs. *Cell Cycle (Georgetown, Tex).* 2008;7(20):3143–3148.
- Fite K, Gomez-Cambronero J. Down-regulation of MicroRNAs (MiRs) 203, 887, 3619 and 182 prevents vimentin-triggered, Phospholipase D (PLD)-mediated cancer cell invasion. *J Biol Chem.* 2016;291(2):719–730. doi:10.1074/jbc.M115.686006
- Shukla KK, Misra S, Pareek P, Mishra V, Singhal B, Sharma P. Recent scenario of microRNA as diagnostic and prognostic biomarkers of prostate cancer. *Urol Oncol.* 2017;35(3):92–101. doi:10.1016/j.urolonc.2016.10.019

13. Zhong J, Liu Y, Xu Q, Yu J, Zhang M. Inhibition of DIXDC1 by microRNA-1271 suppresses the proliferation and invasion of prostate cancer cells. *Biochem Biophys Res Commun*. 2017;484(4):794–800. doi:10.1016/j.bbrc.2017.01.169
14. Liang X, Li H, Fu D, Chong T, Wang Z, Li Z. MicroRNA-1297 inhibits prostate cancer cell proliferation and invasion by targeting the AEG-1/Wnt signaling pathway. *Biochem Biophys Res Commun*. 2016;480(2):208–214. doi:10.1016/j.bbrc.2016.10.029
15. Fujii T, Shimada K, Tatsumi Y, Fujimoto K, Konishi N. Syndecan-1 responsive microRNA-126 and 149 regulate cell proliferation in prostate cancer. *Biochem Biophys Res Commun*. 2015;456(1):183–189. doi:10.1016/j.bbrc.2014.11.056
16. Leung TH, Ching YP, Yam JW, et al. Deleted in liver cancer 2 (DLC2) suppresses cell transformation by means of inhibition of RhoA activity. *Proc Natl Acad Sci U S A*. 2005;102(42):15207–15212. doi:10.1073/pnas.0504501102
17. Ching YP, Wong CM, Chan SF, et al. Deleted in liver cancer (DLC) 2 encodes a RhoGAP protein with growth suppressor function and is underexpressed in hepatocellular carcinoma. *J Biol Chem*. 2003;278(12):10824–10830. doi:10.1074/jbc.M208310200
18. Nagaraja GM, Kandpal RP. Chromosome 13q12 encoded Rho GTPase activating protein suppresses growth of breast carcinoma cells, and yeast two-hybrid screen shows its interaction with several proteins. *Biochem Biophys Res Commun*. 2004;313(3):654–665. doi:10.1016/j.bbrc.2003.12.001
19. Zheng L, Xiang C, Li X, et al. STARD13-correlated ceRNA network-directed inhibition on YAP/TAZ activity suppresses stemness of breast cancer via co-regulating Hippo and Rho-GTPase/F-actin signaling. *J Hematol Oncol*. 2018;11(1):72. doi:10.1186/s13045-018-0613-5
20. El-Sitt S, Khalil BD, Hanna S, El-Sabban M, Fakhreddine N, El-Sibai M. DLC2/StarD13 plays a role of a tumor suppressor in astrocytoma. *Oncol Rep*. 2012;28(2):511–518. doi:10.3892/or.2012.1819
21. Zhang H, Wang F, Hu Y. STARD13 promotes hepatocellular carcinoma apoptosis by acting as a ceRNA for Fas. *Biotechnol Lett*. 2017;39(2):207–217. doi:10.1007/s10529-016-2253-6
22. Li X, Zheng L, Zhang F, et al. STARD13-correlated ceRNA network inhibits EMT and metastasis of breast cancer. *Oncotarget*. 2016;7(17):23197–23211. doi:10.18632/oncotarget.8099
23. Chang S, He S, Qiu G, et al. MicroRNA-125b promotes invasion and metastasis of gastric cancer by targeting STARD13 and NEU1. *Tumour Biol*. 2016;37(9):12141–12151. doi:10.1007/s13277-016-5094-y
24. D'Ippolito E, Plantamura I, Bongiovanni L, et al. miR-9 and miR-200 regulate PDGFR β -mediated endothelial differentiation of tumor cells in triple-negative breast cancer. *Cancer Res*. 2016;76(18):5562–5572. doi:10.1158/0008-5472.CAN-16-0140
25. Su Q, Sena-Esteves M, Gao G. Purification of the recombinant adenovirus by cesium chloride gradient centrifugation. *Cold Spring Harb Protoc*. 2019;2019:5. doi:10.1101/pdb.prot095547
26. Bewig B, Schmidt WE. Accelerated titrating of adenoviruses. *BioTechniques*. 2000;28(5):870–873. doi:10.2144/00285bm08
27. Feldman AT, Wolfe D. Tissue processing and hematoxylin and eosin staining. *Methods Mol Biol*. 2014;1180:31–43.
28. Ashktorab H, Kupfer SS, Brim H, Carethers JM. Racial Disparity in Gastrointestinal Cancer Risk. *Gastroenterology*. 2017;153(4):910–923. doi:10.1053/j.gastro.2017.08.018
29. Kamisawa T, Wood LD, Itoi T, Takaori K. Pancreatic cancer. *Lancet (London, England)*. 2016;388(10039):73–85. doi:10.1016/S0140-6736(16)00141-0
30. Chen W, Zheng R, Zhang S, et al. Cancer incidence and mortality in China in 2013: an analysis based on urbanization level. *Chin J Cancer Res*. 2017;29(1):1–10. doi:10.21147/j.issn.1000-9604.2017.01.01
31. Siegel RL, Miller KD, Jemal A. Cancer statistics, 2018. *CA Cancer J Clin*. 2018;68(1):7–30. doi:10.3322/caac.21442
32. Calin GA, Croce CM. MicroRNA signatures in human cancers. *Nat Rev Cancer*. 2006;6(11):857–866. doi:10.1038/nrc1997
33. Rupaimoole R, Calin GA, Lopez-Berestein G, Sood AK. miRNA deregulation in cancer cells and the tumor microenvironment. *Cancer Discov*. 2016;6(3):235–246. doi:10.1158/2159-8290.CD-15-0893
34. Hirsch FR, Varela-Garcia M, Cappuzzo F. Predictive value of EGFR and HER2 overexpression in advanced non-small-cell lung cancer. *Oncogene*. 2009;28(Suppl 1):S32–37. doi:10.1038/onc.2009.199
35. Gao F, Xiong X, Pan W, et al. A regulatory MDM4 genetic variant locating in the binding sequence of multiple microRNAs contributes to susceptibility of small cell lung cancer. *PLoS One*. 2015;10(8):e0135647. doi:10.1371/journal.pone.0135647

Cancer Management and Research

Publish your work in this journal

Cancer Management and Research is an international, peer-reviewed open access journal focusing on cancer research and the optimal use of preventative and integrated treatment interventions to achieve improved outcomes, enhanced survival and quality of life for the cancer patient.

Submit your manuscript here: <https://www.dovepress.com/cancer-management-and-research-journal>

Dovepress

The manuscript management system is completely online and includes a very quick and fair peer-review system, which is all easy to use. Visit <http://www.dovepress.com/testimonials.php> to read real quotes from published authors.